Int. J. Heat Mass Transfer. Vol. 30, No. 11, pp. 2423–2432, 1987
Printed in Great Britain

0017–9310/87 $3.00 + 0.00

Numerical analysis of mixed convection heat transfer of a high viscosity fluid in a rectangular tank with rolling motion

S. AKAGI and H. KATO
Department of Mechanical Engineering, Osaka University, Suita, Osaka, Japan

(*Received for publication* 1 *May* 1987)

Abstract—A numerical analysis is presented for the mixed convection heat transfer of a high viscosity fluid contained in a two-dimensional rectangular tank subject to rolling motion. The study is motivated by the thermal design of heating systems of a tanker in a wavy sea. Basic equations are given for the body (tank)-fixed coordinate system considering inertia forces acting on the fluid in the tank including centrifugal force, Coriolis force, etc. The isotherms and flow velocity vectors are determined by the numerical solutions of the basic equations. Similarity parameters are introduced, and their influence on the heat transfer is systematically examined.

INTRODUCTION

FLUID motion and heat transfer in a tank with rolling motion are of practical interest since these phenomena appear in heating of oil tanks of tankers which are moving in a wavy sea [1]. The phenomena are characterized by the combined effect of the fluid flows induced by the rolling motion of a tank and the natural convection in it.

Although natural convection in enclosures has been extensively studied in recent years [2–4], the mixed convection heat transfer in an enclosure induced by its rolling motion has received little attention. Studies on the natural convection in an inclined enclosure [5–9] also can be found, but mixed convection in a tank subject to rolling motion has not been treated.

In a previous paper [1], a numerical analysis was presented for the mixed convection in the tank of a tanker subjected to rolling in a wavy sea. Flow patterns and temperature distributions in the tank were given by the results of the numerical solutions of the basic equations describing the fluid motion and heat transfer. In ref. [1] an assumption was made that the motion amplitude was small. Under this assumption equations of fluid motion were represented by the space-fixed coordinate system in order to prevent inertia forces due to the tank motion appearing explicitly in the equations. By introducing the above assumption, however, limitation of the motion amplitude was inevitable in the analysis although the basic equations became simple.

In this study, both equations of motion and energy are represented by the tank-fixed coordinate system to remove limitation of motion amplitude in the analysis. In the equations of motion the inertia forces acting on the fluid in the tank are represented by centrifugal force, Coriolis force, etc. In the study, these inertia forces can be defined in a compact expression which makes the basic equations simple. In the numerical computation of the basic equations, a direct computation with FFT method is introduced to solve the flow–vorticity equation, which can reduce the computer time. The isotherms and flow velocity vectors are then determined by the numerical solutions of the equations. The similarity parameters which define the characteristics of the phenomena are introduced from the basic equations. The influence of the variation of the similarity parameters on the heat transfer is examined systematically for the wide range of rolling motion and natural convection occurring in a tank.

PROBLEM STATEMENT

Mathematical formulation

The geometry of the tank and the heating system under investigation is shown in Fig. 1. The tank is assumed to be two dimensional, and it is completely filled with a viscous fluid. The boundary conditions are that the bottom of the tank is heated, both side walls are cooled, and the tank top is insulated. The tank is assumed to be initially motionless, and the fluid in the tank has an initial uniform temperature T_0. The temperature of the bottom heater is kept at T_w, and that of both side walls of the tank is kept at T_0 during heating.

The natural convection heating is started and continued using a bottom heater. The heating is continued until the mean temperature of the fluid in the tank approaches the average of T_w and T_0. Then, the rolling motion of the tank begins.

The rolling motion of the tank is assumed to be a simple harmonic motion around the tank center 'O' as shown in Fig. 1. The motion amplitude φ of the tank is given by

$$\varphi = -\bar{\varphi}\cos\omega t \qquad (1)$$

NOMENCLATURE

a_x, a_y	inertia forces in x- and y-directions, respectively (equations (2a) and 2(b))
Fr	Froude number, $(\omega l\bar{\varphi})/\sqrt{(gl)}$
g	gravitational acceleration
G	inertia force/gravity force, $\omega^2 l\bar{\varphi}/g$
K	dimensionless viscosity (equation (29))
l	half length of the tank
Nu	Nusselt number (equation (45))
p	pressure of fluid
P	dimensionless pressure, $p/(\rho gl)$
Pr	Prandtl number, $\mu_0/(\rho\alpha)$
Q	heat transfer rate to the tank wall
Ra	Rayleigh number, $\rho g\beta l^3(T_w-T_0)/(\alpha\mu_0)$
Re	Reynolds number, $(\omega l\bar{\varphi})l/\nu$
t	time variable
T	temperature
T^*	similarity parameter for variable viscosity, $(T_w-T_0)/(T_0-T_\infty)$
u, v	velocity components in the x- and y-directions, respectively
U, V	dimensionless velocity components, $u/(\omega l)$, $v/(\omega l)$
W	half width of the heating element
x, y	body (tank)-fixed coordinates
X, Y	dimensionless coordinates, x/l, y/l.

Greek symbols

α	thermal diffusivity of fluid
β	thermal expansion coefficient of fluid
θ	dimensionless temperature, $(T-T_0)/(T_w-T_0)$
$\bar{\theta}$	dimensionless mean temperature in the tank
μ	viscosity of fluid
ν	kinematic viscosity of fluid
ρ	mass density of fluid
$\hat{\rho}$	mass density of fluid under the thermal expansion (equation (7))
τ	dimensionless time, ωt
φ	amplitude of rolling of the tank (equation (1))
$\bar{\varphi}$	maximum amplitude of rolling of the tank
ψ	dimensionless stream function
ω	frequency of rolling motion of the tank
ω^*	dimensionless frequency of rolling motion of the tank, $\omega l^2/\alpha$
Ω	dimensionless vorticity function.

Subscripts

0	cooled surface
w	heated surface
R, L	right and left side of the tank wall, respectively.

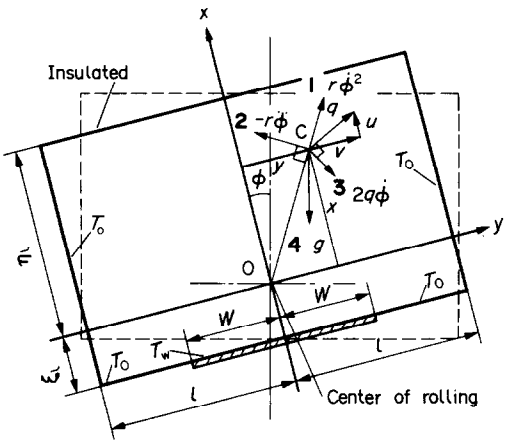

FIG. 1. Calculation model and coordinate system.

where $\bar{\varphi}$ is the maximum amplitude and ω is the motion frequency.

The coordinate system is chosen as the tank-fixed coordinates x–y with the center point 'O' as shown in Fig. 1. The body forces acting on the unit mass of the fluid at the point 'C' in the tank are represented as shown in Fig. 1. They are:

(1) centrifugal force, $r\dot{\varphi}^2$;
(2) inertia force due to angular acceleration, $-r\ddot{\varphi}$;
(3) Coriolis force, $2q\dot{\varphi}(q^2=u^2+v^2)$;
(4) gravitational force, g.

The components a_x and a_y of the above forces in the x- and y-directions are represented by the following equations:

$$a_x = -g\cos\varphi - 2v\dot{\varphi} + x\dot{\varphi}^2 - y\ddot{\varphi} \tag{2a}$$

$$a_y = -g\sin\varphi + 2u\dot{\varphi} + y\dot{\varphi}^2 + x\ddot{\varphi} \tag{2b}$$

where u and v are velocity components corresponding to the coordinates x and y, respectively.

By introducing the expression given in equations (2a) and (2b) the inertia forces acting on the fluid can be defined in a compact form with u, v, φ, $\dot{\varphi}$ and $\ddot{\varphi}$, which will make the equations of fluid motion simple.

The basic equations for the flow and the heat transfer then can be represented with the coordinate system x, y as follows.

The continuity equation:

$$\frac{\partial u}{\partial x} + \frac{\partial v}{\partial y} = 0. \tag{3}$$

The Navier–Stokes equations:

$$\rho\left(\frac{\partial u}{\partial t}+u\frac{\partial u}{\partial x}+v\frac{\partial u}{\partial y}\right)=-\frac{\partial p}{\partial x}+(\hat{\rho}a_x)+2\frac{\partial}{\partial x}\left\{\mu\frac{\partial u}{\partial x}\right\}+\frac{\partial}{\partial y}\left\{\mu\left(\frac{\partial v}{\partial x}+\frac{\partial u}{\partial y}\right)\right\} \quad (4)$$

$$\rho\left(\frac{\partial v}{\partial t}+u\frac{\partial v}{\partial x}+v\frac{\partial v}{\partial y}\right)=-\frac{\partial p}{\partial y}+(\hat{\rho}a_y)+2\frac{\partial}{\partial y}\left\{\mu\frac{\partial v}{\partial y}\right\}+\frac{\partial}{\partial x}\left\{\mu\left(\frac{\partial v}{\partial x}+\frac{\partial u}{\partial y}\right)\right\}. \quad (5)$$

The energy equation:

$$\frac{\partial T}{\partial t}+u\frac{\partial T}{\partial x}+v\frac{\partial T}{\partial y}=\alpha\left(\frac{\partial^2 T}{\partial x^2}+\frac{\partial^2 T}{\partial y^2}\right). \quad (6)$$

The body force terms $(\hat{\rho}a_x)$ and $(\hat{\rho}a_y)$ in equations (4) and (5) are represented by the following expression using Bousinesq approximation:

$$\hat{\rho}/\rho \simeq 1-\beta(T-T_0) \quad (7)$$

where $\hat{\rho}$ represents the density under the thermal expansion due to the temperature difference $(T-T_0)$.

The body force terms $(\hat{\rho}a_x)$ and $(\hat{\rho}a_y)$ then become

$$(\hat{\rho}a_x) \simeq \rho\{1-\beta(T-T_0)\}a_x \quad (8a)$$

$$(\hat{\rho}a_y) \simeq \rho\{1-\beta(T-T_0)\}a_y. \quad (8b)$$

In equations (4)–(6), the density ρ and the thermal diffusivity α of a high viscosity fluid are assumed to be constant because they are almost invariable with temperature [10]. On the other hand, the viscosity μ of a high viscosity fluid varies steeply with temperature [10].

The viscosity–temperature relation for a high viscosity fluid is given by Vogel [10]:

$$\mu=\mu_\infty e^{b/(T-T_\infty)} \quad (9)$$

where μ is the viscosity of a fluid at a temperature T [10]. The constants μ_∞, b and T_∞ depend on the fluid.

The above equations (3)–(6) are transformed into the dimensionless form by using the following expressions:

$$\left.\begin{aligned} &X=x/l, && Y=y/l\\ &U=u/(\omega l), && V=v/(\omega l)\\ &\theta=(T-T_0)/(T_w-T_0), && \tau=\omega t\\ &P=p/(\rho g l), && K=\mu/\mu_0 \end{aligned}\right\} \quad (10)$$

$$\omega^*=\omega l^2/\alpha \quad (11)$$

$$G=\omega^2 l\bar{\varphi}/g \quad (12)$$

$$Pr=\mu_0/(\rho\alpha) \quad (13)$$

$$Ra=\rho g\beta l^3(T_w-T_0)/(\alpha\mu_0) \quad (14)$$

$$\bar{a}_X \equiv a_x/g=\{-\cos(\bar{\varphi}\cos\tau)+G(-2V\sin\tau+X\sin^2\tau-Y\cos\tau)\} \quad (15a)$$

$$\bar{a}_Y \equiv a_y/g=\{-\sin(\bar{\varphi}\cos\tau)+G(-2U\sin\tau+Y\sin^2\tau-X\cos\tau)\}. \quad (15b)$$

Equations (3)–(6) become

$$\frac{\partial U}{\partial X}+\frac{\partial V}{\partial Y}=0 \quad (16)$$

$$\frac{\partial U}{\partial\tau}+U\frac{\partial U}{\partial X}+V\frac{\partial U}{\partial Y}=-\frac{\bar{\varphi}}{G}\frac{\partial P}{\partial X}+\bar{a}_X\left(\frac{\bar{\varphi}}{G}-\frac{Ra\,Pr}{\omega^{*2}}\theta\right)+\frac{2Pr}{\omega^*}\frac{\partial}{\partial X}\left\{K\frac{\partial U}{\partial X}\right\}+\frac{Pr}{\omega^*}\frac{\partial}{\partial Y}\left\{K\left(\frac{\partial V}{\partial X}+\frac{\partial U}{\partial Y}\right)\right\} \quad (17)$$

$$\frac{\partial V}{\partial\tau}+U\frac{\partial V}{\partial X}+V\frac{\partial V}{\partial Y}=-\frac{\bar{\varphi}}{G}\frac{\partial P}{\partial Y}+\bar{a}_Y\left(\frac{\bar{\varphi}}{G}-\frac{Ra\,Pr}{\omega^{*2}}\theta\right)+\frac{2Pr}{\omega^*}\frac{\partial}{\partial Y}\left\{K\frac{\partial V}{\partial Y}\right\}+\frac{Pr}{\omega^*}\frac{\partial}{\partial X}\left\{K\left(\frac{\partial V}{\partial X}+\frac{\partial U}{\partial Y}\right)\right\} \quad (18)$$

$$\frac{\partial\theta}{\partial\tau}+U\frac{\partial\theta}{\partial X}+V\frac{\partial\theta}{\partial Y}=\frac{1}{\omega^*}\nabla^2\theta. \quad (19)$$

Equations (16)–(18) can be transformed into the following form using a vorticity Ω and a stream function ψ by eliminating the pressure term P from equations (17) and (18):

$$\frac{\partial\Omega}{\partial\tau}+U\frac{\partial\Omega}{\partial X}+V\frac{\partial\Omega}{\partial Y}=2G\cos\tau\left(\frac{\bar{\varphi}}{G}-\frac{Ra\,Pr}{\omega^{*2}}\theta\right)+\frac{Ra\,Pr}{\omega^{*2}}\left(\bar{a}_X\frac{\partial\theta}{\partial Y}-\bar{a}_Y\frac{\partial\theta}{\partial X}\right)+\frac{Pr}{\omega^*}\nabla^2(K\Omega)+\frac{2Pr}{\omega^*}A \quad (20)$$

$$\nabla^2\psi=-\Omega \quad (21)$$

where

$$U=\frac{\partial\psi}{\partial Y},\quad V=-\frac{\partial\psi}{\partial X} \quad (22)$$

$$A=\frac{\partial^2 K}{\partial X^2}\frac{\partial U}{\partial X}-2\frac{\partial^2 K}{\partial X\partial Y}\frac{\partial U}{\partial X}-\frac{\partial^2 K}{\partial Y^2}\frac{\partial V}{\partial Y}. \quad (23)$$

If the viscosity is invariable, then the values of K and A become $K=1$ and $A=0$.

Equations (20)–(23) are solved together with equation (19) under the given initial and boundary conditions.

Similarity parameters

The similarity parameters defined by equations (11)–(14) are explained as follows.

(1) $\omega^*=\omega l^2/\alpha$. The parameter ω^* represents the dimensionless angular frequency of rolling motion, which is expressed from equation (11) as

$$\omega^*=\{(\omega l\bar{\varphi})l/\nu\}(\nu/\alpha)(1/\bar{\varphi})\equiv Re\cdot Pr/\bar{\varphi} \quad (24)$$

where Re is Reynolds number, defined by

$$Re=(\omega l\bar{\varphi})l/\nu. \quad (25)$$

The parameter Pr/ω^* in equation (20) represents $1/Re$, which appears in a Navier–Stokes equation of a usual forced flow.

(2) $G = \omega^2 l\bar{\varphi}/g$. The parameter G represents the ratio of the angular acceleration relative to the gravity g. The value G represents the Froude number Fr of the rolling motion by replacing it in the following expression:

$$G = \omega^2 l\bar{\varphi}/g = \{\omega^2 l^2 \bar{\varphi}^2/(gl)\}(1/\bar{\varphi}) = Fr^2(1/\bar{\varphi}) \quad (26)$$

where Fr represents the Froude number

$$Fr = (\omega l\bar{\varphi})/\sqrt{(gl)}. \quad (27)$$

The amplitude $\bar{\varphi}$ also represents one of the similarity parameters.

(3) *Ra, Pr and* Ra/ω^{*2}. The parameters Ra and Pr are the Rayleigh number and the Prandtl number which appear in the case of usual natural convection. The parameter Ra/ω^{*2} indicates the relative importance of natural/forced convection as appears in equations (17) and (18), or (20), namely

$$Ra/\omega^{*2} = (Ra/Re^2)(1/Pr^2)\bar{\varphi}^2. \quad (28)$$

When the value of Ra/ω^{*2} becomes small, the importance of the body force term including $\partial\theta/\partial Y$ and $\partial\theta/\partial X$ in equation (20) is reduced. Then, the heat transfer is influenced mainly by the forced flow, i.e. the rolling motion, where the flow is characterized by the values of $\bar{\varphi}$ and ω^*.

(4) $K = \mu/\mu_0$. The parameter K represents the dimensionless viscosity–temperature relation of the fluid which is introduced by equation (9), namely

$$K = \frac{\mu}{\mu_0} = \left(\frac{\mu_w}{\mu_0}\right)(1+T^*)\theta/(1+T^*\theta) \quad (29)$$

where μ_w and μ_0 represent viscosities corresponding to the temperatures T_w and T_0 respectively.

The dimensionless temperature T^* in equation (29) is given by

$$T^* = (T_w - T_0)/(T_0 - T_\infty). \quad (30)$$

The parameters μ_w/μ_0 and T^* in equation (29) are similarity parameters which define the influence of viscosity variation with temperature on heat transfer.

Initial and boundary conditions

The initial conditions for equations (20)–(23) and (19) are determined from the pure natural convection condition before the oscillation begins, where the mean temperature $\bar{\theta}$ in the tank has approached the average of T_w and T_0, i.e. $\bar{\theta} \simeq 0.5$. The calculation for the pure natural convection is similar to that in a previous paper [1], and therefore the details of the calculation are omitted here.

The boundary conditions are determined by the assumption that the relative velocity components are zero at the tank walls. The thermal boundary conditions are given by Fig. 1, as mentioned previously.

(I) $Y = -1$ (at the left wall shown in Fig. 1):

$$U = V = 0, \quad \psi = 0, \quad \theta = 0. \quad (31)$$

(II) $Y = 1$ (at the right wall):

$$U = V = 0, \quad \psi = 0, \quad \theta = 0. \quad (32)$$

(III) $X = -\xi$ (at the tank bottom):

$$U = V = 0, \quad \psi = 0$$
$$\theta = 1 \text{ (heated surface)} \quad (33)$$
$$\theta = 0 \text{ (cooled surface).}$$

(IV) $X = \eta$ (at the tank top):

$$U = V = 0, \quad \psi = 0$$
$$\partial\theta/\partial X = 0 \text{ (insulated).} \quad (34)$$

In this case, the center of rolling 'O' was assumed to be the center of the tank, namely $\xi = \eta = 1$.

PARAMETER SELECTION AND SOLUTION PROCEDURE

Parameter selection

The high viscosity fluid selected for the calculation was a COM (coal oil mixture), a fuel alternative consisting of pulverized coal and heavy fuel oil [10]. The viscosity–temperature relation of a COM is similar to typical heavy fuel oils.

The values of the constants b, μ_∞ and T_∞ in equation (9) for a COM [10] are

$$\mu_\infty = 5.86 \times 10^{-1} \text{ [N s m}^{-2}\text{]}$$
$$b = 110.6 \text{ [K]} \quad (35)$$
$$T_\infty = 275.35 \text{ [K]}.$$

The temperatures of the tank walls are chosen to be $T_w = 423.2$ K [150°C] and $T_0 = 303.2$ K [30°C]. Using these values, μ_w/μ_0 and T^* in equation (29) become $\mu_w/\mu_0 = 1/25.1$ and $T^* = 4.3$, respectively.

The values of the similarity parameters Ra, Pr, ω^*, G and $\bar{\varphi}$ which appear in equations (20)–(23) and (19) are systematically changed to examine the influence of these parameters on the fluid motion and heat transfer in the tank, as will be explained later.

Solution procedure

Equations (20)–(23) and (19), with the initial and boundary conditions given by equations (31)–(34), are solved with a time-marching, finite difference technique. Forward time and central space differences are used except for the convection terms in equations (19) and (20), for which upwind differencing is employed. The calculation proceeds by explicitly advancing θ and Ω with difference forms of equations (19) and (20). A difference form of equation (21) is then solved for the new ψ field by a direct computation using the following Fourier series expansion (FFT) method.

In the solution, the terms ψ and Ω in equation (21) are represented as follows:

$$\psi(X, Y) = \sum_{n=1}^{\infty} B_n(Y) \sin\left(\frac{n\pi X}{2}\right) \quad (36)$$

$$B_n(Y) = \frac{2}{2\times 1}\int_{-1}^{1} \psi(X, Y) \sin\left(\frac{n\pi X}{2}\right) dX \quad (37)$$

$$\Omega(X, Y) = \sum_{n=1}^{\infty} D_n(Y) \sin\left(\frac{n\pi X}{2}\right) \quad (38)$$

$$D_n(Y) = \frac{2}{2\times 1}\int_{-1}^{1} \Omega(X, Y) \sin\left(\frac{n\pi X}{2}\right) dX. \quad (39)$$

Substituting equations (35) and (37) into equation (21), the following equation is introduced:

$$-\left(\frac{n\pi X}{2}\right)^2 B_n(Y) + \frac{d^2 B_n(Y)}{dY^2} = -D_n(Y)$$

$$(n = 1, 2, \ldots). \quad (40)$$

When the term $D_n(Y)$ is calculated by equation (39) for the given value of Ω, the value of $B_n(Y)$ is determined by equation (40). The new ψ field is then given by equation (36). The calculation is conducted by using the FFT algorithm. Velocities and vorticities are obtained from the new ψ field using finite difference approximations. Since all fields are then known, the calculations can proceed by further time advancement.

RESULTS

Values of the similarity parameters

The values of Ra, Pr, ω^*, G and $\bar{\varphi}$ are selected in the calculations as follows. The values of $Pr = 10^3$ and $Ra = 10^8$ are fixed, and the values of ω^*, G and $\bar{\varphi}$ are varied for the following cases (1) and (2).

(1) The value ω^* (or Ra/ω^{*2}) is varied for $G = 0.1$:

$$\omega^* = 10^4, 10^5, 3\times 10^5, 5\times 10^5, 10^6 \quad (41)$$

$$[Ra/\omega^{*2} = 1, 10^{-2}, (1/9)\times 10^{-3}, (1/2.5)\times 10^{-3}, 10^{-4}]. \quad (42)$$

(2) The value G is varied for the two kinds of values of ω^* and $\bar{\varphi}$:

$$G = 0.01, 0.05, 0.2 \text{ (for } \omega^* = 3\times 10^5, \quad \bar{\varphi} = 25°) \quad (43)$$

$$G = 0.3, 10 \text{ (for } \omega^* = 5\times 10^6, \quad \bar{\varphi} = 30°). \quad (44)$$

Although the values ω^* for an actual ship reach the order of $\omega^* = 10^8$–10^9, the values for the calculation were taken to be in the range of $\omega^* = 10^4$–10^6, i.e. $Re = \omega^*\bar{\varphi}/Pr \simeq 5$–$5\times 10^2$, because the calculation model was restricted to the laminar flow case.

Flow and temperature fields

The computed flow fields and temperature fields in the tank are first shown. Figure 2 illustrates the calculated isotherms and velocity vectors in the tank during rolling for $Ra = 10^8$, $Pr = 10^3$, $\omega^* = 10^6$, $G = 0.1$ and $\bar{\varphi} = 25°$.

In Fig. 2, individual graphs from the top to the bottom in the figure pertain to a time sequence. The top graph illustrates the result of the pure natural convection case, where the heating continues until the mean temperature in the tank reaches about $\bar{\theta} = 0.5$. It is observed that the heated plume flows up unsymmetrically from the bottom heater toward the tank top, then it flows down along each side of the tank. Although the boundary conditions given by equations (31)–(34) are symmetrical about the center line of the tank $Y = 0$, the isotherms and the velocity vectors in Fig. 2(1) are not symmetrical. The reason for this is that the flows due to heating by the horizontal bottom surface of the tank are unstable, and they tend to move to one side of the heating surface [11].

The temperature in the tank becomes nearly uniform except in the layers near the tank walls and heating surface, where the temperature changes steeply. At this point, the rolling motion of the tank is initiated.

In Fig. 2, conditions for rolling are shown to the left of the figure, isotherm fields to the center and flow velocity vector fields to the right. In this figure, a time sequence from $\tau = \pi/4$ (the second graph) to 10π (the bottom graph) is shown. Figure 2 also shows that reciprocal circulating flows relative to the motion of the tank are found. They change their directions of circulation as the motion of the tank reverses. The isotherms fluctuate from side to side in the tank as the flow changes its circulating direction. A core part is formed in the center of the tank which is motionless during the rolling of the tank.

Influence of similarity parameters

In order to examine influence of changing similarity parameters, the heat transfer rate and Nusselt numbers at the tank wall were calculated for a number of cases.

(1) *Influence of* ω^*. Figures 3(1)–(3) illustrate the dimensionless mean temperature $\bar{\theta}$ in the tank, the heat transfer rate to each side wall, Q_R or Q_L, the respective Nusselt number Nu_R or Nu_L, and the total rate of the heat transfer of both side walls, $Q = Q_R + Q_L$, by changing $\omega^* = 10^6$–10^4 for $Ra = 10^6$, $Pr = 10^3$, $G = 0.1$ and $\bar{\varphi} = 25°$. These values are expressed as functions of the dimensionless time variable τ as shown in Fig. 3. The mean temperature $\bar{\theta}$ in the tank was calculated by averaging the temperature Q_{ij} at each mesh point i, j.

The heat transfer rates to the side wall of the tank, Q_R or Q_L, were calculated using the numerical values of the temperature gradient at the wall $\partial\theta/\partial Y|_{R,L}$:

$$Q_{R,L} = \frac{1}{2}\int_{-1}^{1} \left.\frac{\partial\theta}{\partial Y}\right|_{R,L} dX. \quad (45)$$

The Nusselt numbers are given using $Q_{R,L}$ and $\bar{\theta}$:

$$Nu_{R,L} = Q_{R,L}/\bar{\theta}. \quad (46)$$

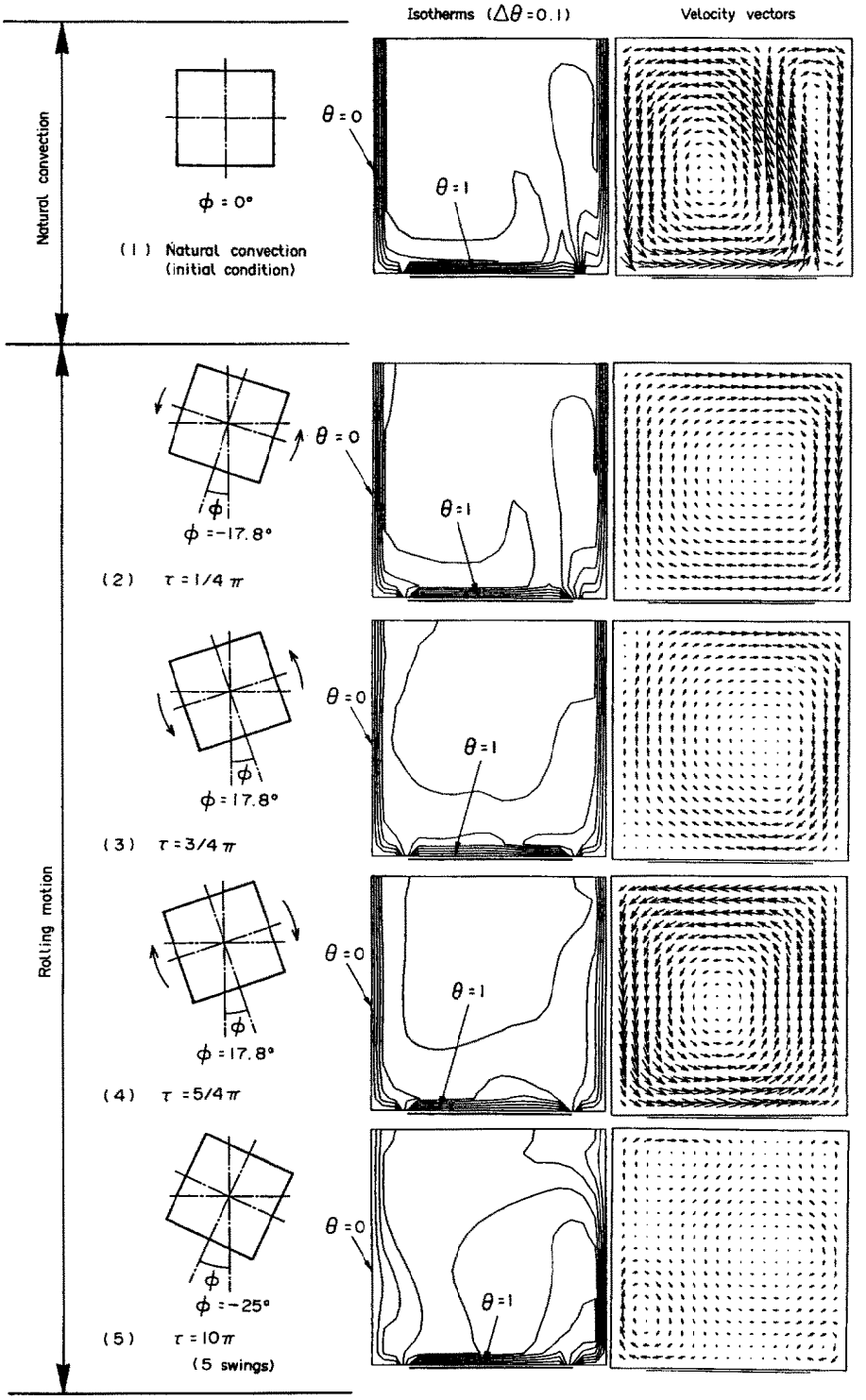

FIG. 2. Time sequence of isotherms and flow velocity vectors in the tank during natural convection and rolling motion ($\omega^* = 10^6$; $Ra = 10^8$; $Pr = 10^3$; $G = 0.1$; $\bar{\varphi} = 25°$).

As shown in Fig. 3(1), the heat transfer rates Q_R and Q_L, as well as the Nusselt numbers Nu_R and Nu_L, oscillate regularly due to the rolling motion of the tank. The mean temperature $\bar{\theta}$ in the tank decreases slightly as the rolling motion continues. The reason for this phenomenon is considered in the following discussion.

The fluid selected for the calculation is accompanied

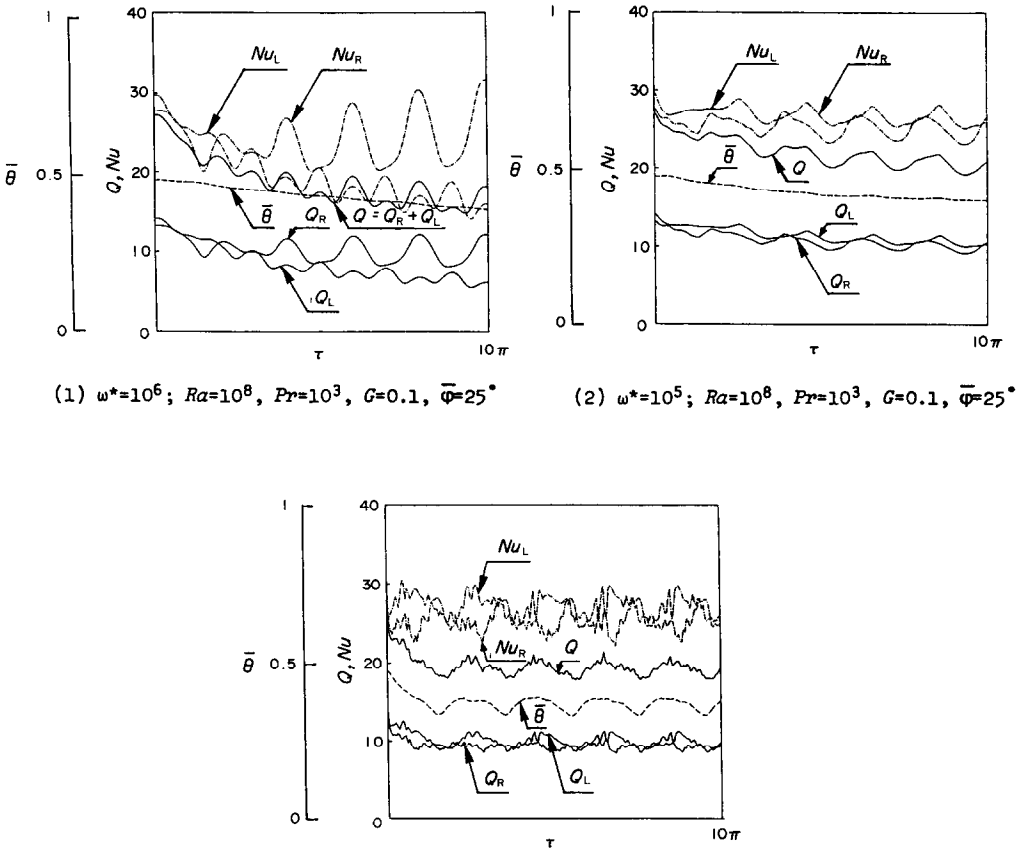

FIG. 3. Heat transfer rate Q to the tank side wall, mean temperature $\bar{\theta}$ in the tank and Nusselt number Nu at the tank wall during rolling motion.

by a strong viscosity dependence on temperature. Before rolling begins, the heat transfer by pure natural convection is promoted near the building surface due to the lowered viscosity as a result of the higher temperature. When rolling begins, the cooled fluid with higher viscosity near the side wall flows down to the heating surface, which would prevent the heat transfer to the fluid. The above effect results in a decrease in heat transfer from the heating surface, which causes also a decrease in the mean temperature of the fluid in the tank during rolling. In Fig. 3(1) the heat transfer rates Q_R and Q_L seem to decrease slightly as the rolling motion continues, which is considered to be due to the fact that the cooled fluid with higher viscosity becomes thicker and thicker at the tank walls, preventing the heat transfer from the fluid to the tank walls.

In Figs. 3(2) and (3), the same calculations were done by changing the values of ω^* to 10^5 and 10^4, respectively. In the case of $\omega^* = 10^5$ shown by Fig. 3(2), the heat transfer rate to the tank wall and the mean temperature in the tank are essentially similar to the case shown by Fig. 3(1), although the amplitudes of fluctuation of Q and Nu are reduced in this case. In the case of Fig. 3(3), where the value of ω^* is reduced to 10^4, the heat transfer rates fluctuate chaotically. This phenomenon is caused by interaction between the natural convection flows and the flows due to the rolling motion of the tank, where the rolling is weaker than the cases shown by Figs. 3(1) and (2). In this case, the value of Ra/ω^{*2}, which indicates the relative importance of natural convection, reaches the order of 1. This means that the strengths of both phenomena are mutually comparable.

Figure 4 illustrates the velocity vectors and isotherms in the tank corresponding to Fig. 3(3). In this case, the flows in the tank seem unstable and fluctuate as shown by the velocity vectors, where the flows up and down interact mutually. As shown in Fig. 4, the flows along both side vertical walls always tend downwards. They are caused by natural convection due to cooling of the walls. These phenomena are different from the case of Fig. 2, where the flows form the reciprocal circulating pattern relative to the tank motion, which is mainly influenced by the rolling motion of the tank.

(2) *Influence of G.* Figures 5(1) and (2) illustrate the heat transfer rate to the tank wall and the mean temperature in the tank, where the value of G is varied from $G = 0.01$ to 0.2 for $\omega^* = 3 \times 10^5$, $Ra = 10^8$,

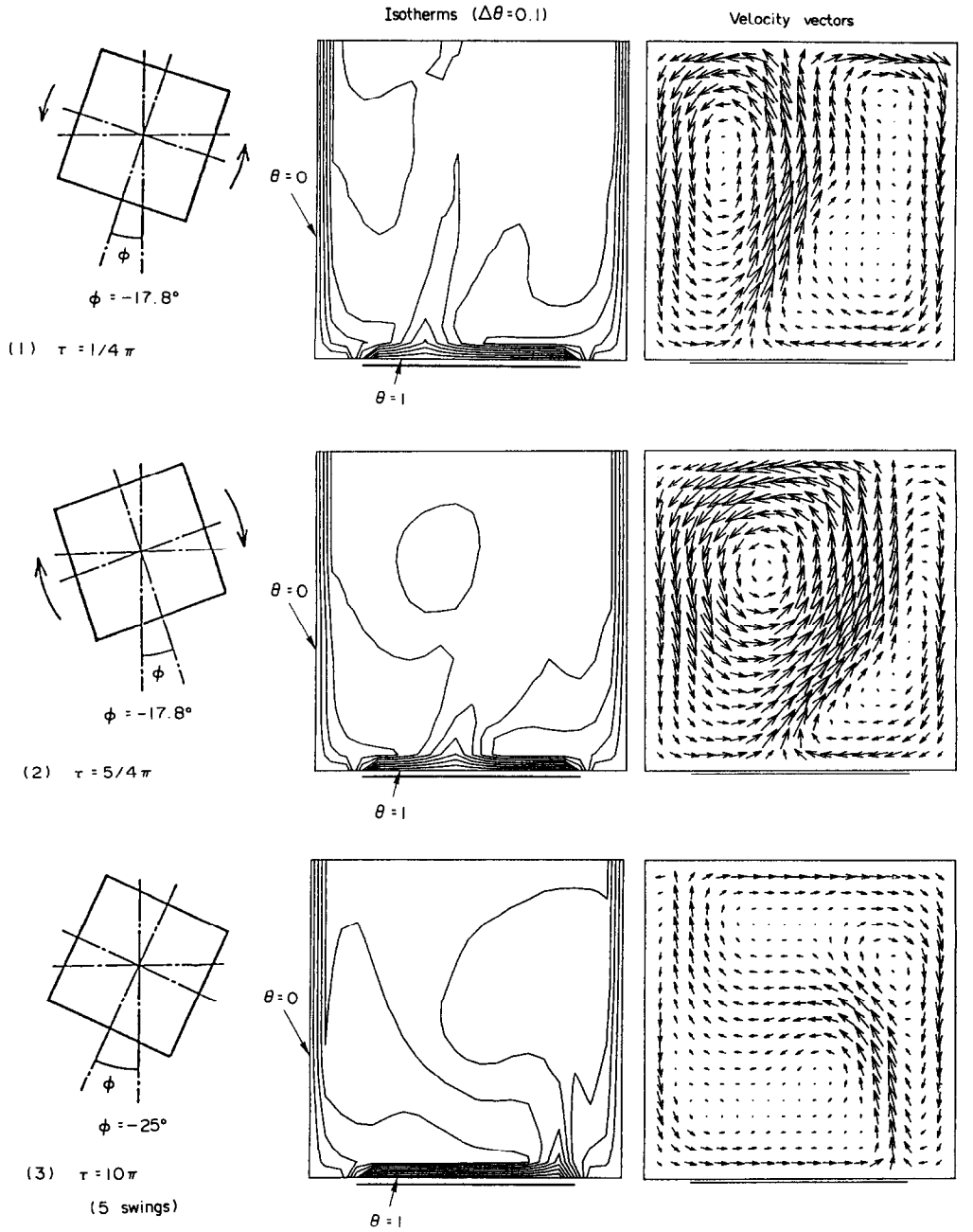

FIG. 4. Time sequence of isotherms and flow velocity vectors in the tank during rolling motion ($\omega^* = 10^4$; $Ra = 10^8$; $Pr = 10^3$; $G = 0.1$; $\bar{\varphi} = 25°$).

$Pr = 10^3$ and $\bar{\varphi} = 25°$. A comparison of Figs. 5(1) and (2) indicates that there exists little difference in the heat transfer rates between the cases $G = 0.2$ and 0.01. This means that the influence of G on the convection flows is weak. It is considered that this is due to the fact that the flows due to the rolling are little influenced by Froude number, $Fr = \sqrt{(\bar{\varphi}G)}$, because the tank has no free surface of the fluid in these cases. If there exists a free surface in the tank, the motion of the fluid during rolling would be much influenced by the value of Fr, namely the variation of G, which would also cause the heat transfer.

(3) *Influence of* $\bar{\varphi}$. Lastly, the influence of the amplitude of the rolling $\bar{\varphi}$ is examined by increasing the value of $\bar{\varphi}$ from $\bar{\varphi} = 25°$ to 30°. Figure 6 illustrates the heat transfer rate and the mean temperature in the tank, where the value of $\bar{\varphi}$ is taken as $\bar{\varphi} = 30°$ for $\omega^* = 5 \times 10^6$, $Ra = 10^8$, $Pr = 10^3$, and $G = 0.3$ and 10. It is observed that the amplitudes of oscillation of Q and Nu shown in Fig. 6 increase to some degree

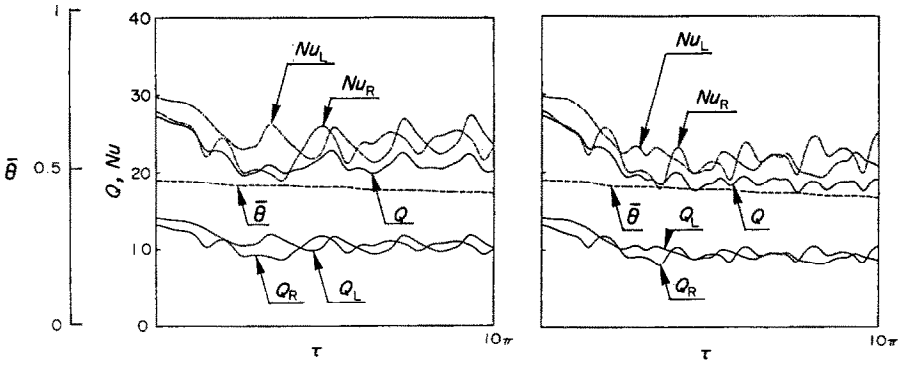

(1) G=0.2; ω^*=3×10^5, Ra=10^8, Pr=10^3, $\bar{\varphi}$=25° (2) G=0.01; ω^*=3×10^5, Ra=10^8, Pr=10^3, $\bar{\varphi}$=25°

FIG. 5. Heat transfer rate Q to the tank side wall, mean temperature $\bar{\theta}$ in the tank and Nusselt number Nu at the tank wall during rolling motion.

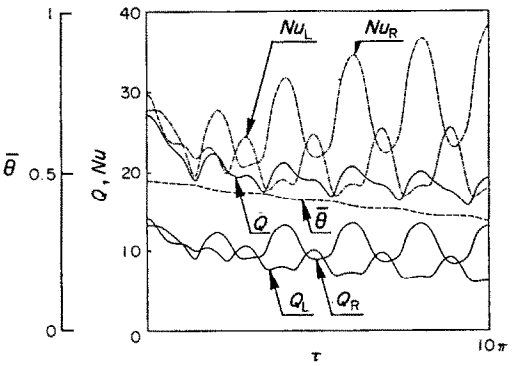

FIG. 6. Heat transfer rate Q to the tank side wall mean temperature $\bar{\theta}$ in the tank and Nusselt number Nu at the tank wall during rolling motion (G = 0.3 and 10; $\bar{\varphi}$ = 30°; $\omega^* = 5 \times 10^6$; $Ra = 10^8$; $Pr = 10^3$).

compared with the result shown in Fig. 3(1), where $\bar{\varphi}$ is taken to be 25°, although the patterns of oscillation are not very different.

The calculations were also done by increasing the value of G to 10. As shown in Fig. 6, no difference is found between both results of G = 0.3 and 10. This can be expected from the aforementioned result of Fig. 5.

The above results provide a systematical understanding of the phenomena of the mixed convection heat transfer in a tank which is subjected to rolling motion with a wide range of motion amplitude $\bar{\varphi}$ and frequency ω^*.

SUMMARY

Mixed convection heat transfer in a tank subjected to rolling motion has been studied numerically. The motivation of the study was to understand the heat transfer process which appears in heating oils stored in ship's tanks of a tanker which is rolling in a wavy sea.

The results are summarized as follows.

(1) The basic equations of fluid motion in a tank are defined using the body (tank)-fixed coordinate systems considering inertia forces including centrifugal force, Coriolis force, etc. These forces are defined in a compact expression which makes the basic equations simple.

(2) The isotherms and velocity vector fields are determined from the numerical solutions of the basic equations. The heat transfer rate to the tank wall is also calculated.

(3) Similarity parameters which define the fluid flows and heat transfer in a tank are introduced from the basic equations. The influence of their variation on the convection is systematically examined for the wide range of amplitude and the frequency of rolling motion of the tank.

(4) When the value of dimensionless frequency ω^* of the rolling is larger than 10^5, the heat transfer in the tank is influenced mainly by the rolling, while it is influenced by both natural convection and the rolling motion when the value of ω^* is reduced to $\omega^* = 10^4$.

(5) The influence of the Froude number $Fr = \sqrt{(\bar{\varphi}G)}$ on the heat transfer is weak because the fluid in the tank is assumed to have no free surface.

The above results are not only helpful for the thermal design of a heating system of oil tankers, but also are useful as an aid to understanding the heat transfer phenomena in a tank subjected to rolling motion.

REFERENCES

1. S. Akagi and K. Uchida, Fluid motion and heat transfer of a high viscosity fluid in a rectangular tank of a ship with oscillating motion, *J. Heat Transfer, ASME* (to appear).
2. S. Ostrach, Natural convection in enclosures. In *Advances in Heat Transfer* (Edited by J. P. Hartnett and T. F. Irvine, Jr.), Vol. 8, pp. 161–227. Academic Press, New York (1972).
3. I. Catton, Natural convection in enclosures, *Proc. 6th Int. Heat Transfer Conf.*, Toronto, Vol. 6, pp. 13–31. Hemisphere, Washington, D.C. (1978).
4. K. E. Torrance and I. Catton (Editors), *Natural Con-*

vection in Enclosures, ASME, HTD-Vol. 8 (1980).
5. H. Ozoe, H. Sayama and S. W. Churchill, Natural convection in an inclined square channel, *Int. J. Heat Mass Transfer* **17,** 401–406 (1974).
6. J. N. Arnold, I. Catton and D. K. Edwards, Experimental investigation of natural convection in inclined rectangular regions of differing aspect ratios, *J. Heat Transfer, ASME* **98,** 67–71 (1976).
7. S. J. M. Linthorst, W. M. M. Schinkel and C. J. Hoogendoorn, Flow structure with natural convection in inclined air filled enclosures, *J. Heat Transfer, ASME* **103,** 535–539 (1981).
8. H. Ozoe, K. Fujii, N. Lior and S. W. Churchill, Long rolls generated by natural convection in an inclined rectangular enclosure, *Int. J. Heat Mass Transfer* **26,** 1427–1438 (1983).
9. S. Acharya and R. J. Goldstein, Natural convection in an externally heated vertical or inclined square box containing internal energy sources, *J. Heat Transfer, ASME* **107,** 855–866 (1985).
10. S. Akagi and K. Yoshitani, A study on heat transfer during natural convective heating of a coal oil mixture (COM), *Heat Transfer—Japanese Research*, Vol. 11, pp. 1–26. Scripta, Washington, D.C. (1982).
11. S. Akagi, K. Uchida and M. Takemura, A computer simulation of the natural convection of a high viscosity fluid contained in a two-dimensional rectangular tank, *Trans. JSME (Ser. B)* **52,** 609–616 (1986).

ANALYSE NUMERIQUE DE LA CONVECTION THERMIQUE MIXTE D'UN FLUIDE TRES VISQUEUX, DANS UN RESERVOIR RECTANGULAIRE AVEC UN MOUVEMENT DE ROULEMENT

Résumé—Une analyse numérique est présentée pour la convection thermique mixte d'un fluide à haute viscosité, contenu dans un réservoir bidimensionnel rectangulaire, soumis à une rotation. L'étude est motivée par la conception des systèmes de chauffage d'un tanker en mer agitée. Des équations de base sont données pour un système de coordonnées fixé au réservoir, en considérant les forces d'inertie incluant les forces centrifuges, la force de Coriolis, etc. Les isothermes et les vecteurs vitesses sont déterminés par la résolution numérique des équations de base. Des paramètres de similitude sont introduits et leur influence sur le transfert thermique est systématiquement examinée.

NUMERISCHE UNTERSUCHUNG DER WÄRMEÜBERTRAGUNG DURCH MISCHKONVEKTION EINER SEHR ZÄHEN FLÜSSIGKEIT IN EINEM RECHTECKIGEN TANK BEI ROLLENDER BEWEGUNG

Zusammenfassung—Es wird eine numerische Untersuchung der Wärmeübertragung durch Misch-Konvektion einer sehr zähen Flüssigkeit in einem zweidimensionalen rechteckigen Tank, der einer rollenden Bewegung unterworfen ist, vorgestellt. Anlaß der Studie ist die thermische Auslegung von Heizungssystemen eines Tankers in unruhiger See. Für das körper(Tank-)feste Koordinatensystem werden die grundlegenden Gleichungen angegeben. Sie berücksichtigen Trägheitskräfte, welche auf die Flüssigkeit im Tank wirken, einschließlich Zentrifugalkraft und Corioliskraft, etc. Die Isothermen und die Strömungsgeschwindigkeitsvektoren werden mittels numerischer Lösung der Grundgleichungen bestimmt. Ähnlichkeitsparameter werden eingeführt und ihr Einfluß auf die Wärmeübertragung systematisch untersucht.

ЧИСЛЕННЫЙ АНАЛИЗ ПЕРЕНОСА ТЕПЛА СМЕШАННОЙ КОНВЕКЦИЕЙ В ПРЯМОУГОЛЬНОМ ЗАПОЛНЕННОМ ВЫСОКОВЯЗКОЙ ЖИДКОСТЬЮ РЕЗЕРВУАРЕ ПРИ ЕГО КОЛЕБАНИЯХ ОТНОСИТЕЛЬНО ПРОДОЛЬНОЙ ОСИ

Аннотация—Проведен численный анализ переноса тепла смешанной конвекцией в двумерном, прямоугольном, заполненном высоковязкой жидкостью резервуаре, совершающем колебания относительно продольной оси. Исследование выполнено для расчета работы нагревательной системы танкера в условиях неспокойного моря. Представлены основные уравнения для системы координат, связанной с танкером, с учетом инерционных сил, действующих на жидкость в замкнутом объеме, включая центробежную силу, силу Кориолиса и т.д. С помощью численных решений основных уравнений определены изотермы и векторы скорости течения. Введены параметры подобия и проведено систематическое исследование их влияния на теплообмен.